J Mater Sci: Mater Med (2011) 22:1027–1036
DOI 10.1007/s10856-011-4255-1

The effect of substrate topography on hFOB cell behavior and initial cell adhesion evaluated by a cytodetacher

Shih-Ping Yang · Tzer-Min Lee

Received: 10 November 2010 / Accepted: 6 February 2011 / Published online: 18 February 2011

Abstract This study examined human fetal osteoblast (hFOB) cell morphology, adhesion force, and proliferation on a titanium-coated grooved surface. V-shaped grooves with a depth of 2.4 μm (T1) or 4.8 μm (T2) were produced in silicon wafers using photolithography and wet etching techniques. The grooved substrates were coated with a 200-nm-thick layer of titanium using a sputtering system. Smooth Ti-coated Si wafers were used as control surfaces. Analysis of the scanning electron microscopy observations shows that the cells responded to the micropattern by spreading out and becoming elongated. The MTT (3-(4,5-dimethylthiazol-2-yl)-2,5-diphenyltetrazolium bromide) assay indicated that the grooved specimens had a significantly larger number of cells than did the control group after 5- and 15-day cultures. The cytocompatibility of specimens was quantitatively evaluated by a cytodetacher, which directly measures the detachment shear force of an individual cell to the substrate. After 30-min culture, the cell adhesion forces were 48.4, 136.6, and 103.3 nN for the smooth specimen, the T1 specimen, and the T2 specimen, respectively. The cell adhesion strengths were 294, 501, and 590 Pa for the smooth specimen, the T1 specimen, and the T2 specimen, respectively. The cell adhesion force and cell adhesion strength indicate the quality of cell adhesion, explaining the largest number of cells on grooved specimens. The experimental results suggest that the grooved patterns affect the cell shape and cytoskeletal structure, and thus influence the cell proliferation and cell adhesion force. The cytodetachment test with nanonewton resolution is a sensitive method for studying cell–biomaterial interaction.

S.-P. Yang · T.-M. Lee (✉)
Institute of Oral Medicine, National Cheng Kung University, Tainan 701, Taiwan, ROC
e-mail: tmlee@mail.ncku.edu.tw

1 Introduction

For dental implants, shape design and surface properties are the major factors of implant success, especially in bone healing in the early and long-term periods [1]. Various studies have indicated that the surface properties of implant, such as surface chemistry and surface topography, are key factors which mediate bone cell responses in the early stage [2]. Therefore, the surface properties of artificial implants have been investigated to maximize biocompatibility. Generally, the topography of the surface profoundly affects the shape of cells. A previous study indicated that surface topography influences cellular responses from the early stage adhesion and migration and thus regulates the physiological response of cells [3]. Furthermore, topography regulates cell growth, gene expression, the secretion of proteinases, differentiation, and even life and death [4–8]. Schneider et al. [9] suggested that osteoblast gene expression and mineralization are affected by roughened implant surface microtopographies during the osseointegration of dental implants. In vivo examination revealed that the fixation of dental implants might be improved by the incorporation of macroscopic features or micro features [10].

For in vitro tests, the cytocompatibility of biomaterials depends on the cell morphology, cell growth, and the state of differentiation cells. The diversity of cell responses is used to distinguish different kinds of biomaterials or their treatments. However, the sensitivity of traditional in vitro biological tests is sometimes too low to discriminate the subtle changes in specimens. Atomic force microscopy (AFM) can be used to characterize cell adhesion and to quantify the adhesion force in the piconewton range [11]. The cell adhesion force can thus be used to evaluate the

cell response to surfaces with various properties in the initial stage of cell behavior.

When a tissue cell comes into contact with implants, it perceives the chemistry of the surface using integrin transmembrane proteins in order to find suitable sites for adhesion, spreading, motility, growth, and maturation [12]. Cell adhesion is involved in various natural phenomena such as embryogenesis, the maintenance of tissue structure, wound healing, immune response, metastasis, and the tissue integration of biomaterials [13]. Therefore, cell adhesion is important because it is the first step of attachment to materials and leads to subsequent cell responses. Light microscopy combined with anti-body staining is usually employed to observe and characterize cell adhesion. High-resolution electron microscopy is suitable for observation of adhesion sites and underlying protein networks.

Several methods have been proposed for evaluating the cell adhesion force [14–17]. In our previous study, a cantilever-based technique was used to measure the adhesion force of osteoblasts cultured on various kinds of surface-treated titanium alloy disk [18]. This method directly measures the actual strength of attachment between a single cell and its substrate to better assess the cytocompatibility of biomaterials. The micropatterned substrate can control cell behavior and even induce a switch from growth to apoptosis [8]. Multiple-groove substrates have been used by several authors as a model patterned biomaterial for investigating the interaction of anchorage-dependent cells with topography. In the present study, the effect of topography on cell behavior was analyzed using a quantitative detachment method to understand the fundamental principle of cell adhesion. The cell shape was controlled using a Ti-coated microgrooved surface and a cytodetacher was used to evaluate the initial adhesion force of osteoblasts. In addition, the cell morphology, area, elongation, and proliferation were measured to evaluate osteoblast behavior on the microgrooved surface.

2 Materials and methods

2.1 Microfabrication of Ti-coated grooved pattern

Silicon (Si) wafers with the ⟨100⟩ p-type crystal orientation were purchased from Wafer Work Corporation, Taiwan. All grooved silicon substrates were fabricated using photolithography and wet etching techniques at National Nano Device Laboratory, Tainan, Taiwan. After the RCA cleaning process was employed to remove the native oxide layer on the Si wafer, a high-temperature oven was used to grow a SiO_2 layer on the silicon substrate. The pattern on the photomask was transferred onto the positive-resist-coated silicon wafer by photolithography. The pattern on the sample was then etched to the desired dimensions using an anisotropic etchant. The various grooves used in the experiments were obtained by varying the etching conditions. After sonication in isopropanol and acetone, the micropatterns were coated with a 200-nm-thick titanium layer using a sputtering system (Duratek Model 101, Taiwan). In order to remove the residual gas in chamber, the process chamber was evacuated to a base pressure lower than 10^{-7} Torr. High purity argon (99.9995%) gas was then back-filled into the chamber until a working pressure of 8 mTorr was obtained. The substrates were sputter-cleaned with argon using a substrate bias. The deposition parameters were 2 min, 10 sccm argon gas, and 1,000 W. After the sputtering process, the smooth Ti-coated substrates and the grooved Ti-coated substrates were cut into 5 mm × 5 mm specimens and then ultrasonically cleaned in acetone and deionized water for 5 min, respectively. Two kinds of V-shape grooved pattern were used in this investigation: (a) the T1 coating pattern (T1-CP) had 2.4-μm-deep grooves with a 4.6 μm pitch comprising a 1.3-μm-wide ridge and a 3.3-μm-wide groove, and (b) the T2 coating pattern (T2-CP) had 4.8-μm-deep grooves with a 10.5 μm pitch comprising a 3.8-μm-wide ridge and a 6.7-μm-wide groove. Smooth Ti-coated Si wafers were used as control surfaces.

The surface and cross-section morphologies and composition of specimens were analyzed using a scanning electron microscope (SEM, Jeol 6390LV, Japan) attached with an energy dispersive spectrometer (EDS, Oxford 350, England). The phase of the coating was identified using a thin-film X-ray diffractometer (Rigaku D/Max2500, Japan) with CuK_α radiation, operated at 40 kV, 1 mA, an incident angle of 2°, and a scan speed of 4° (2θ)/min.

2.2 Cell culture

The human fetal osteoblast line (hfOB1.19, ATCC number: CRL-11372 was obtained from the American Type Culture Collection (ATCC, Rockville, MD, USA). The hFOB1.19 cell line was maintained in Dulbecco's modified Eagle's medium with F12 (DMEM + F12, GIBICO) containing 10% fetal calf serum (FBS, GIBICO) and 0.3 g/l of G418 (GIBICO) in an atmosphere of 5% CO_2/95% air at 34°C to control the pH value. The medium was changed every 2 days. After reaching confluence, the cells were washed with phosphate-buffered saline (PBS), treated with 0.05% trypsin–EDTA (GIBICO), and centrifuged at 1,000 rpm for 10 min. After sterilization, each specimen was placed in one well of a 24-well plate (Nunclon Nalge Nunc Int., Denmark). For each test, there were five specimens in each group ($N = 5$). Before seeding, all specimens were packed in autoclaving bags, steam sterilized at 121°C for 30 min,

dried at 121°C for 15 min, and then placed into the 24-well plates.

2.3 Cell morphology, area, and elongation

After sterilization, each specimen was placed in one well of the 24-well plate. The cell suspension was seeded on the specimens at a density of 5×10^3 cells/cm^2 for 30 min, 1 h, and 3 h. 500 μl of the medium was then added to each well. The samples were washed three times with PBS, and fixed with 2.5% glutaraldehyde at 4°C, 4% OsO_4 at 37°C, and 1% tannic acid at 4°C. The samples were dehydrated with a series of graded ethanol solutions and immersed in hexamethyldisilazane (HMDS SIGMA) for 10 min. Finally, after being sputter-coated with gold, the specimens were observed by SEM at an acceleration voltage of 20 kV. After SEM observation at low magnification, the images was analyzed by ImageJ (Version 1.41, National Institutes of Health). For cell area and perimeter calculations, 50–60 cells were used for cell area calculations. The length and breadth of cells were defined by the longest chord and longest chord perpendicular to the length, respectively. The cell elongation index was defined as the ratio of the length to the breadth of each cell.

2.4 Cell adhesion force

The cytodetacher was modified with a microscope working station and laser tweezers (Cell Robotics Inc, Albuquerque, NM, USA). The adhesion strength between substrates and cells was measured by the cytodetacher (Fig. 1), which has four major components: (a) cell selector, (b) SPM cantilever tip (Anosensors NanoWorld AG, Switzerland), (c) sample holder, and (d) microscope working station equipped with a motorized stage, a video camera, and a microscope (Nikon, model TE300) [21]. The whole system was operated in a closed plastic chamber containing 5% CO_2 at 37°C. hFOB cells were seeded onto the specimens at a density of 5×10^3 cells/cm^2 for 30 min. After the end of the culture, the samples were placed into the sample holder with 10 ml of DMEM without phenol red at 37°C. In the test, the cytodetacher manipulated the AFM cantilever tip, which detached individual cells. Sequential images of the cytodetachment process were recorded at 20 frames per second. The maximum deflection of the cantilever tip was calculated using Matlab 7.0 (The MathWorks, Inc., USA) and applying Hooke's law as follows:

$$F_{\text{adhesion}} = K \times \delta_{\max}$$

where $\delta_{\max}$ is the maximum deflection and F_{adhesion} is the cell adhesion force. $K = 0.019$ N m^{-1} is the spring constant, determined from experiments [19].

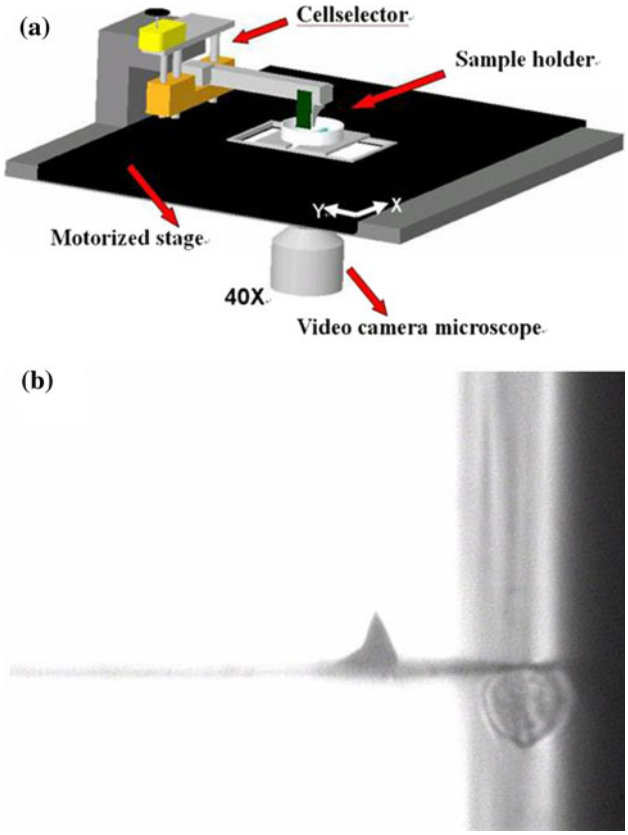

Fig. 1 **a** Major components of the cytodetacher apparatus and **b** acquired image [21]

2.5 Cell proliferation

The cells were seeded on the specimens at a density of 10^4 cells/cm^2 for 5 and 15 days, respectively. Osteoblasts were cultured in the tissue culture and polystyrene (PS) served as controls. The culture medium was changed every 2 days during culture. At harvest, the samples were treated with 3-(4,5-dimethylthiazol-2-yl)-2,5-diphenyltetrazolium bromide (MTT, GIBICO) for 4 h in 37°C, and then with dimethylsulfoxide (DMSO, Sigma) for 30 min. The working solutions were evaluated using an enzyme-linked immunosorbent assay (ELISA) plate reader (Tecan, Sunrise) at a wavelength of 562 nm against a reference wavelength of 650 nm.

2.6 Statistics

Each measurement was the mean ± standard deviation, and the analysis of one-way variance (ANOVA) was used to evaluate the significance of differences. Differences were considered significant at $p \leq 0.05$.

3 Results

3.1 Characterization of micropattern

The SEM cross-section morphologies of the Ti-coated groove pattern are shown in Fig. 2a and b. The results indicate that the etching process produced a groove with wall slope at a 55″ angle to form a complete V shape. The SEM/EDS analysis of the chemical composition shows that the specimens are mainly composed of Ti and the silicon substrate (Fig. 2c). The existence of silicon can be explained by the depth of EDS. In this study, the thickness of the Ti coating was 200 nm, but the depth of EDS is more than 1 μm at an acceleration voltage of 20 kV. Figure 3 shows the thin-film X-ray diffraction pattern of the Ti coatings. The XRD pattern is characteristic of Ti in accordance with the standard XRD pattern (JCPD 44-1294).

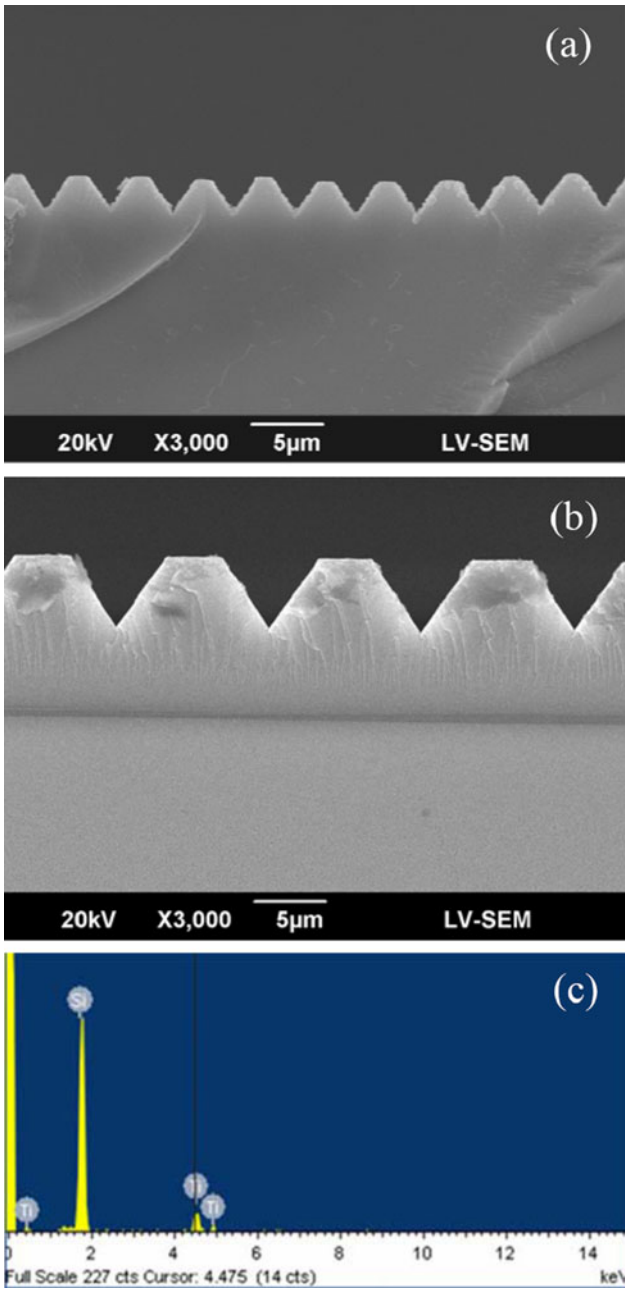

Fig. 2 SEM micrographs of Ti-coated pattern used in this study: **a** cross-section morphology of T1-CP, **b** cross-section morphology T2-CP. The ridge/groove/depth dimensions of patterns are 1.3/3.3/2.4 μm for T1-CP and 3.8/6.7/4.8 μm for T1-CP. **c** EDS analysis confirming that the 200-nm-thick coating was composed of Ti element. The Si element is a component of the substrate (Si wafer)

3.2 Cell morphology, area, elongation

After the 30-min culture, the hFOB cell morphologies on the surface of specimens were observed by SEM (see Fig. 4). In Fig. 4a, the cell is spherical in shape with no apparent sign of filopodia on the smooth surface. In contrast, the filopodia of the hFOB cell extends to the neighboring ridge on the T1-CP specimen (Fig. 4b). For the T2-CP specimen, the hFOB cell attaches to the Ti-coated micropattern surface, and the filopodia of the cell extends to the ridge and grooves (Fig. 4c). The SEM results suggest that hFOB cells on the micropattern specimens have better spreading and adhesion morphologies than those on smooth specimens after 30-min culture.

Figure 5a–c shows SEM micrographs of hFOB cells cultured on smooth and grooved specimens after 1-h culture. On the smooth specimens, the cell morphology had filopodia extending from the central area (Fig. 5a). On the T1-CP specimen, hFOB cells reacted to the grooved pattern by becoming aligned in the direction of the grooves (Fig. 5b). Compared to cells on the T1-CP specimen, cells on the T2-CP specimen had a less flat and less aligned morphology (Fig. 5c). When the culture time was increased to 3 h, the hFOB cells flattened and spread on the smooth surface (Fig. 6a). On the two kinds of Ti-coated grooved surface, the cells became elongated on the patterns (Fig. 6b, c).

The results of average cell area for the smooth and micropatterned specimens for various culture periods are shown in Fig. 7. As shown in the figure, the average cell area of each sample increased significantly over time for all specimens ($P < 0.05$). After 30-min, 1-h, and 3-h cultures, the average cell area for the T1-CP specimen was significantly larger and smoother than that of the T2-CP specimen ($P < 0.001$). No significant difference was found between the smooth and T2-CP group.

Figure 8 shows that there was a significant increase in cell elongation as a function of culture period for smooth and grooved specimens ($P < 0.05$). After culture of 30 min, the elongation indices are 1.12, 1.34, and 1.26 for the smooth specimen, T1-CP, and T2-CP, respectively. There was no statistical difference found among the three

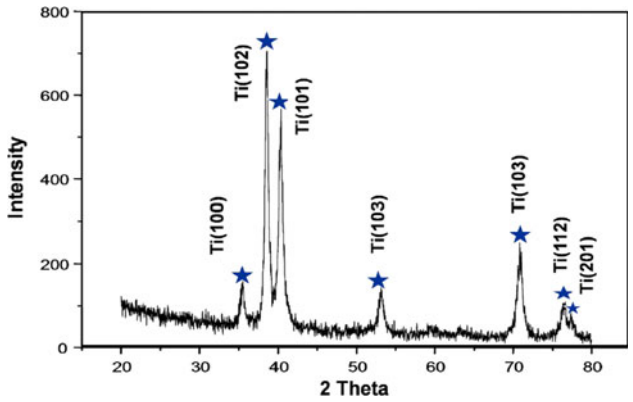

Fig. 3 X-ray diffraction pattern of Ti coating. A crystalline Ti structure was formed in the sputtering process

kinds of specimen. Compared to the smooth substrate, the cell elongation indices of grooved surfaces were significantly higher for 1-h and 3-h culture periods ($P < 0.0001$). Consistent with cell morphology (Fig. 5), cell elongation on the T1-CP specimen was statistically higher ($P < 0.001$) than that on the T2-CP specimen for 1-h and 3-h culture periods.

3.3 Cell adhesion force

Figure 9 shows the adhesion force between an individual hFOB cell and the substrate surface obtained by a cyto-detacher. The cell adhesion forces are 48.4, 136.6, and 103.3 nN for the smooth specimen, T1-CP, and T2-CP, respectively. Compared to the smooth specimen, the patterned specimens had significantly higher cell adhesion forces, as obtained from ANOVA analysis ($P < 0.001$). In addition, the T1-CP exhibited a statistically higher level of hFOB cell adhesion force than that of T1-CP at 30-min culture period ($P < 0.01$).

3.4 Cell proliferation

The proliferation data of the hFOB cells on the smooth and grooved specimens are presented in Fig. 10. The figure shows that the number of cells increased with culture time for all specimens. Statistical evaluation of the proliferation data revealed a significant difference between the smooth surface and the grooved specimens after 5-day and 15-day culture periods ($P < 0.001$). The number of cells on the surface of T1-CP was significantly higher than that for T2-CP after 5 and 15 days of culture ($P < 0.01$).

4 Discussion

Previous studies have suggested that the underlying substrate topography influences cell behavior, including

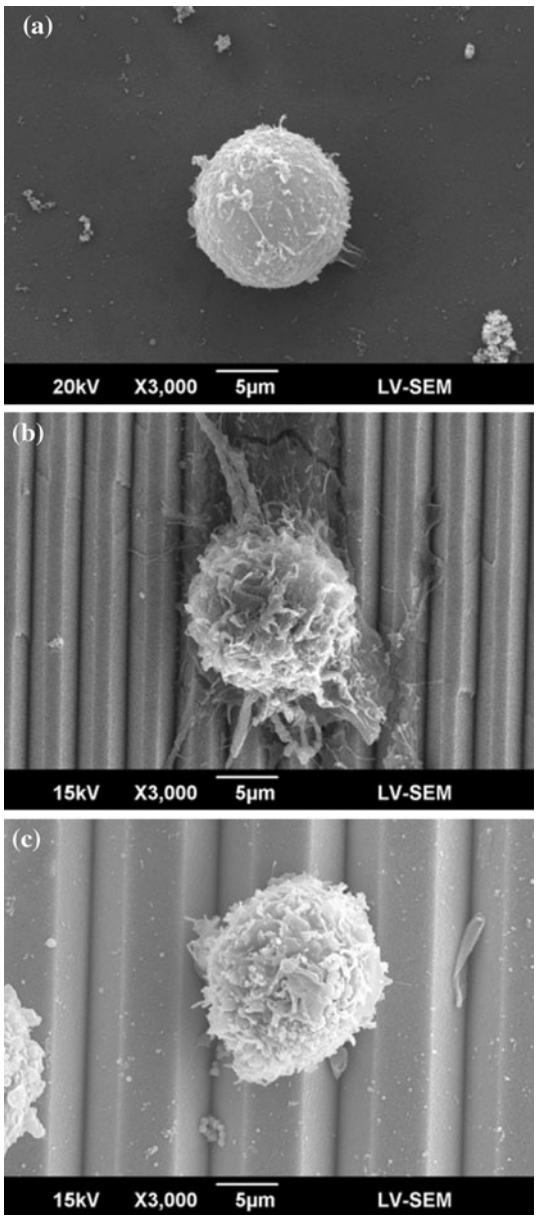

Fig. 4 SEM micrographs of hFOB cells cultured for 30 min on **a** a smooth specimen, **b** T1-CP, and **c** T2-CP. On the T1-CP specimen, the cell is spherical with early signs of filopodial extension to a neighboring ridge

proliferation, migration, and adhesion, via direct and indirect interactions [2, 20, 21]. Corneal epithelial cells interact with a complex basement membrane composed of proteoglycans, collagen fibers, and multi-adhesive matrix proteins which form a rich three-dimensional structure with characteristic nanoscale dimensions [22]. In the present study, Ti-coated specimens with uniform parallel surface micro-grooves were used to study the effect of the grooves on cell–surface interactions. The human fetal osteoblast 1.19 (hFOB 1.19) cells are conditionally immortalized with a gene coding a temperature-sensitive mutant (tsA58) of

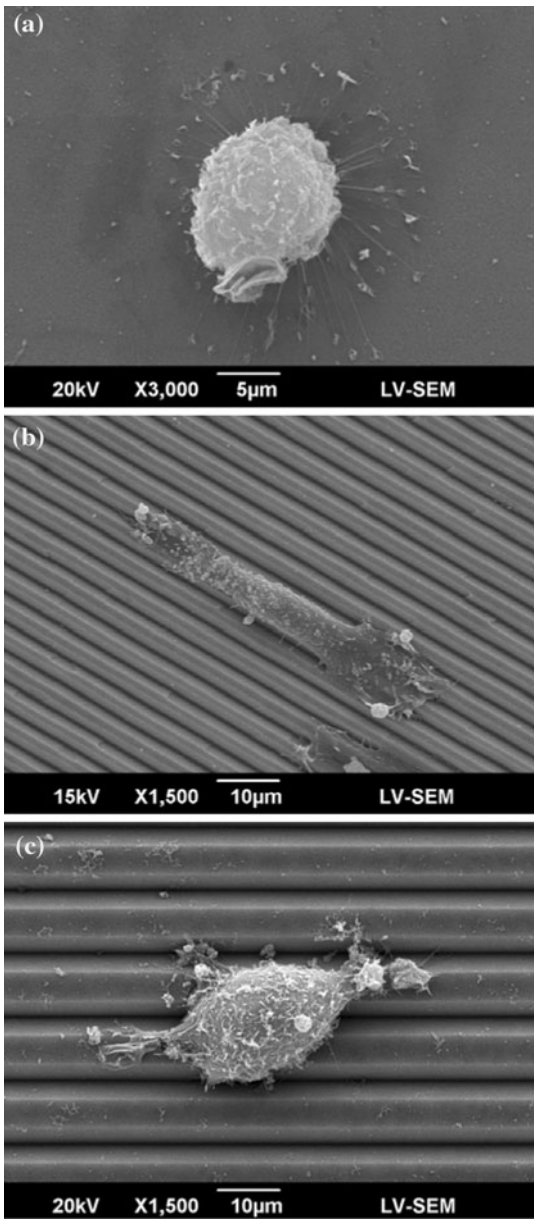

Fig. 5 SEM micrographs of hFOB cells cultured for 1 h on **a** a smooth specimen, **b** T1-CP, and **c** T2-CP. On the T1-CP specimen, the cell became elongated in the direction of the groove

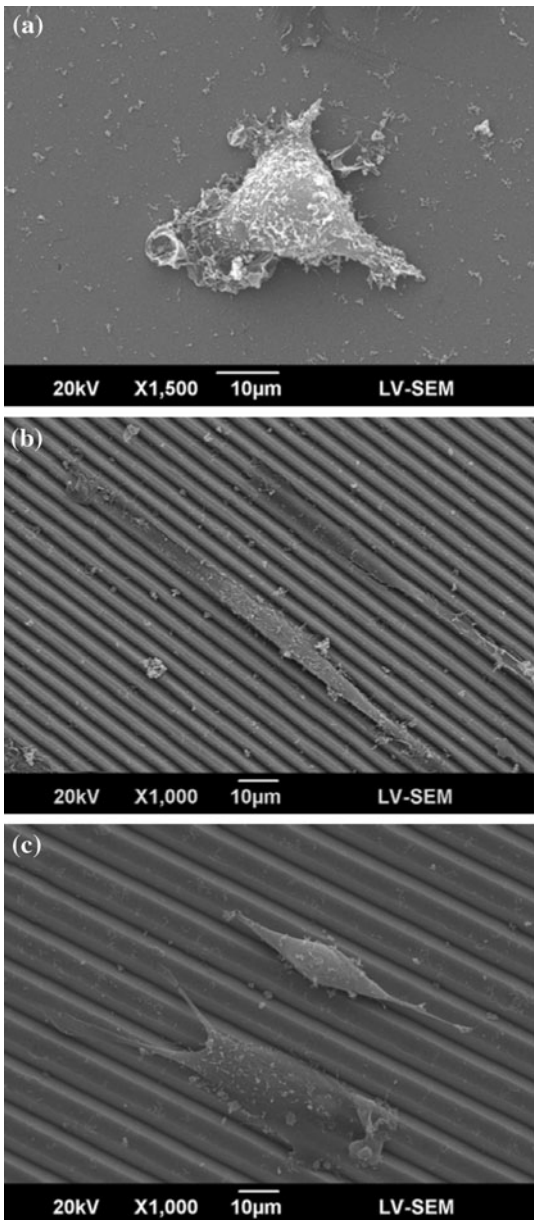

Fig. 6 SEM micrographs of hFOB cells cultured for 3 h on **a** a smooth specimen, **b** T1-CP, and **c** T2-CP. On the grooved surfaces, cells exhibit a flat elongated morphology along the groove. Randomly spread cells appear on the smooth substrate

the SV40 large T antigen. Cells cultured at the permissive temperature of 33.5°C undergo rapid cell proliferation. Therefore, the hFOB cells are suitable for evaluation biocompatibility in orthopaedic applications. The hFOB cell behavior, such as cell morphology, area, elongation, and proliferation, can be controlled by the topography of the surface in contact with cells. In particular, the effect of topography on the cell–specimen adhesion force was quantitatively and directly measured by a cytodetacher.

Several investigations reported that cellular-substrate interaction is associated with the surface topography, chemical composition, surface energy, and surface charge of biomaterials [23–25]. These surface characteristics determine the adsorption of biological molecules and the structure rearrangement of adsorbed molecules on the surface of biomaterials [23–25]. Furthermore, these adsorbed molecules determine the initial cell attachment, adhesion, and spreading [23–25]. A previous study found that osteoblasts attached but failed to spread without serum [26]. In contrast, the cells developed focal adhesion or stress fibers with serum, resulting in rapid attachment and good spreading.

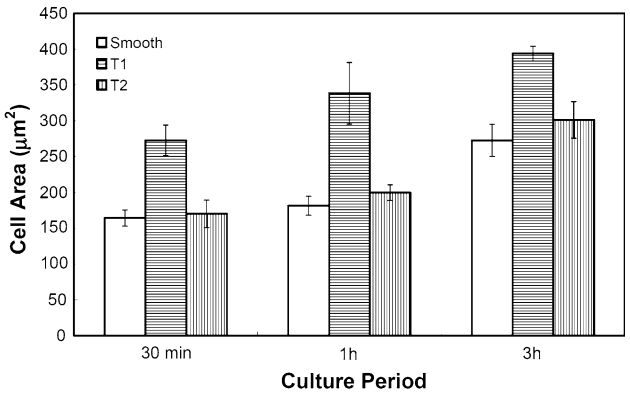

Fig. 7 Effect of surface topography on average cell area. The T1-CP specimens have a significantly higher average cell area than those of the smooth and T2-CP specimens ($P < 0.001$). Values are in mean ± SD

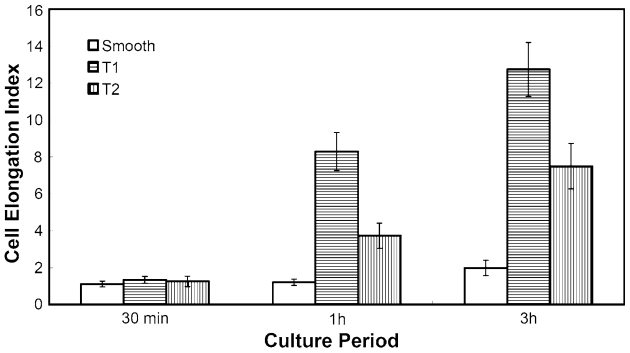

Fig. 8 Effect of surface topography on the cell elongation index. After 1-h and 3-h cultures, the value can be ranked in the following decreasing order: T1-CP, T2-CP, smooth specimen ($P < 0.001$). Values are in mean ± SD

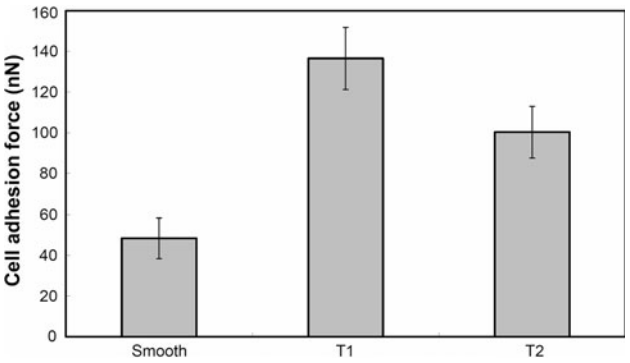

Fig. 9 Adhesion force of hFOB cell to smooth, T1-CP, and T2-CP specimens for 30-min culture. The values can be ranked in the following decreasing order: T1-CP, T2-CP, smooth specimen ($P < 0.001$). Values are in mean ± SD

In the present study, the micropatttern was fabricated by lithography and etching processes, and a Ti coating was deposited on the surface by a sputtering process. The surface composition was disregarded because the Ti coating was

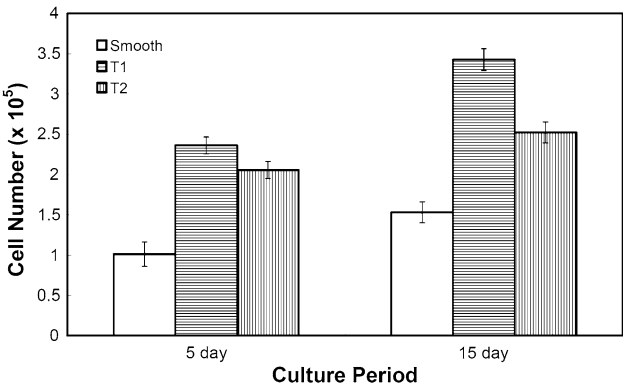

Fig. 10 Cell proliferation of hFOB cells on various specimens. The numbers of cells can be ranked in the following decreasing order: T1-CP, T2-CP, smooth specimen ($P < 0.01$). Values are in mean ± SD

uniform on both the smooth and grooved specimens. The surface morphology of Ti-coated specimens is discussed in relation to their biological behavior, such as cell morphology, area, elongation, adhesion force, and proliferation. The results of SEM observation indicate a significant difference between the morphology of hFOB cells on the smooth and grooved specimens, implying that surface morphology affects cellular response during the early phases.

A study of bovine aortic endothelial cells cultured on poly(dimethylsiloxane) (PDMS) substrates showed that grooved substrates guided intracellular F-actin and focal adhesions to align parallel to the channel direction after 1-h culture [27]. Contact guidance has been observed on osteoblastic cells. Isolated bone cells from neonatal rat calvaria on a smooth polystyrene (PS) substrate were found to align themselves in an end-to-end fashion parallel to the direction of the grooved pattern, and an increased ordering of confluent regions of cells and extracellular matrix was observed on the grooved surface [28].

In cell adhesion, mature focal adhesion is elongated structures and mostly oriented in the direction of the main stress fibres. Balaban et al. [29] found that the force of cell exerts, via actomyosin contraction, at its focal adhesion determines their assembly, on a time scale below seconds. It can be assumed that a cell generates the force on its adhesion molecules is sufficient to induce a 'feedback response' by locally modulating molecular interactions. The cell could use its own contractile apparatus to regulate adhesion in a rapid and local fashion, directing the response exactly to the location at which force must be applied, namely to the binding sites to a rigid surface or to distinguish between substrates with different rigidities. The influence of ridge width, groove width, and groove depth on cells is also considered. The relative role of ridges and grooves in the process of alignment appears to differ depending on the cell type, such as neuron fibroblast,

epithelium, macrophages, neutrophils, and osteogenic cells [30–32]. Walboomers et al. [33] suggested that the depth of the groove is the main determining factor in the alignment of fibroblast along the surface microgrooves. Chesmel et al. [28] found that bone cells oriented along a 5-μm grooved surface, but that they ignored the surface topography with a 0.5-μm groove pattern.

As shown in Fig. 8, the cell elongation index of the grooved surface is more than 3.5 after 1-h culture, but the elongation index on the smooth specimens is lower than 2 even after 3-h culture. The results suggest that Ti-coated grooves alter cell shape, making it possible to influence the long-term cell behavior and function. The experimental results also indicate that the Ti-coated grooved substrate had a higher cell adhesion force and more cells than did the smooth specimens. The cell elongation index was significantly higher for the 2.4-μm-deep-groove T1-CP specimen than that of the T2-PC specimen with 4.8-μm-deep grooves. The results reveal that 2.4 μm is deep enough to elongate hFOB cells on a Ti-coated grooved substrate. The higher cell elongation index for the T1-CP specimen is due to the 1.3-μm-wide ridge on T1-CP limiting the breadth of hFOB cells and increasing the length of cells compared to the T2-PC specimen with 3.8-μm-wide ridges. The SEM results also indicate a more rapid cell elongation on the T1-CP specimen.

In general, the initial adhesion of cells to the substrate belongs to the first phase of cell/biomaterial interaction, and the quality of the first phase influences the cell proliferation and differentiation on biomaterials. For example, grooves altered cell shape, and regulated mRNA and the extracellular-matrix (ECM) protein fibronectin of an in vitro culture of human fibroblasts on a micromachined grooved surface [34]. Schneider et al. showed that a microgrooved surface of commercially pure titanium can alter the regulation of osteoblast differentiation by influencing the level of gene expression of key osteogenic factors, such as Cbfa1 and BSPII. In the present study, the hFOB cells belong to anchorage-dependent cells, which require an adhesive surface to exert force and consequently spread. The surface topography may influence the cell proliferation. As shown in Fig. 10, the grooved specimens had a significantly higher number of cells than did smooth specimens for 5-d and 15-d cultures. In addition, the number of cells for T1-CP was significantly higher than that for T2-CP after 5 and 15 days of culture. The difference in cell shape possible affected cell proliferation on the different micropatterns. On T1-PC specimens, the early adhesion increased the cell area, which is related to the contact area between the cell and substrate. It is believed that a higher cell-to-substrate contact area increases the cell adhesion force to the substrate. Cytodetachment tests show that the T1-CP specimen had significantly higher hFOB cell adhesion than that of the T2-CP specimen for the 30-min culture.

Cells consist of four basic elements: the cell envelope, cytoskeleton, nucleus, and cytosol. The cytoskeleton is a dynamic structure that provides mechanical stability, maintains cell shape, protects the cell, and plays an important role in cellular division. Chen et al. [7] studied the effect of a micropatterned surface on the cell shape and function. They found that the micropatterned substrate could control the spread of human and bovine capillary endothelial cells, and that the cells were switched from growth to apoptosis. The mechanical signals, such as cytoskeletal structure and focal adhesion complex, associated with changes in cell shape along with chemical signals could lead to shape- and adhesion-dependent cell survival and growth, the characterization of cell adhesion force could be further studied to understand the adhesion properties. Several researchers have measured cell affinity using methods such as centrifugation [13], shear stress facility-based techniques [14], and cantilever-based technique [15, 16, 35]. However, only the cantilever-based technique is capable of directly assessing the cell adhesion strength by detaching individual cells from the surface of the specimen. For example, a spinning disk device could apply a linear range of forces to attach cells on specimens. Although this apparatus allows the quantitative analysis of cell adhesion under uniform and constant surface chemical conditions, the adhesion force could only represent the normally distributed attachment property of the cell population. According to previous studies, the cell adhesion strength is very sensitive to cell–biomaterial interaction, such as contact area, adsorbed proteins, culture time, and cell shape [36–38]. The adhesion strength of rat osteosarcoma cells (ROS 17/2.8) on fibronectin adsorbed onto bioactive glass or borosilicate control glass was three-fold higher than that of cells on bioactive and non-reactive glass [37]. Cytodetachment results show that the initial hFOB cell adhesion force ranged from 48.4 to 136.6 nN after 30 min of incubation. Yamamoto et al. cultured murine fibroblast L929 on a glass dish for 24 h and found that the shear adhesion force ranged from 310 to 390 nN by applying a lateral load using a micro-cantilever system [16]. The adhesion force of individual chondrocytes cultured on a polymer surface ranged from 8 to 50 nN for 8-h, 12-h, 24-h, and 5-day cultures [38]. For our experiments, the measured adhesion force ranged from a few to hundreds of nN, which is consistent with values reported by other researchers.

As shown in Fig. 10, the cell adhesion forces were 48.4, 136.6, and 103.3 nN for the smooth specimen, T1-CP, and T2-CP after 30-min culture, respectively. The results can be attributed to the topography of the specimens. After adhesion to the substrate, the cells arranged their

cytoskeleton to exert force against their adhesive contacts and to structurally support the cell interiors. SEM observation shows that the micropattern could control the cell shape and then change the cell area and elongation index, which indicates different cytoskeletal structures. As shown in Fig. 7, the average cell areas were 164, 273, and 170 μm^2 for the smooth specimen, T1-CP, and T2-CP, respectively. The higher cell adhesion force for T1-CP can be explained by the larger cell adhesion area. The study of Yamamoto et al. indicated that cells with a larger cell adhesion area tend to need larger forces to be detached from the glass surface.

It is interesting that there was no significant difference between the cell areas of the smooth and T2-CP specimens. Although the elongation indices of the smooth and T2-CP specimens are similar after 30-min culture, the cells on the T2-CP specimen tended to elongate in the direction of the grooves compared to the randomly flat cell morphology on the smooth specimen after 1-h and 3-h cultures. The elongated cell morphology on the T2-CP specimen shows that its cytoskeletal structure is different than that of the smooth specimen. The cells on the T2-CP specimen had better cell adhesion area and cell adhesion force than those of the smooth specimen.

Cell adhesion strength is also an important parameter for evaluating cell adhesion quality. The cell adhesive strength is defined as the cell adhesion force divided by cell adhesive area. In the present study, the values of cell adhesion strength were 294, 501, and 590 Pa for the smooth specimen, T1-CP, and T2-CP, respectively. The values of cell adhesion strength are not constant among the three types of specimen, which disagrees with the results of the study by Yamamoto et al. In their study, the cell adhesion strength tended to be constant irrespective of the size of the cell adhesive area on the glass substrate. The cell adhesion strength represents the quality of the cell adhesion on a substrate, the micropattern alters the cytoskeletal structure, which further changes the quality of cell adhesion.

The present study is a pilot-study of evaluating the cell affinity for grooved patterns and the ability to control cell shape. The experimental system is a sensitive method for quantifying and analyzing cell adhesion to substrates. For biomaterials such as artificial dental implants or artificial hip joints, the shear strength of cell–biomaterial adhesion is important because a shear force acts on the interface between cells and the implanted device under a loading condition. In addition, our results provide insight into how grooved patterns influence cell response in terms of the cell adhesion force, morphology, area, elongation, and proliferation. These results can be used to design the surface morphology of implants in clinical applications. The cytoskeleton and osteogenic markers, such as osteocalcin or osteopontin, are also important to investigate single cell adhesion. As to further study, the effect of micropattern on cytoskeleton and osteogenic markers still need further investigation.

5 Conclusion

The effect of Ti-coated groove patterns on the cell morphology, area, elongation, adhesion, and proliferation was investigated. SEM results show that hFOB cells on a grooved surface have better spreading and adhesion morphologies than those on smooth specimens. For grooved specimens, T1-CP had a higher hFOB cell area and elongation index than those of T2-CP, which indicates surface topography affects the cell behavior in this study. The grooved pattern also altered hFOB cell proliferation after 5- and 15-day cultures. The proliferation of hFOB cells on grooved specimens is significantly higher than that on smooth specimens. Cells cultured on the grooved specimens had stronger initial adhesion forces and cell adhesion strengths. The high cell adhesion to a grooved surface resulted from an enhancement in the elongation of cell shape. A previous study found that a micropatterned substrate can mediate cell adhesion and control cell growth and viability. In the present study, the micropattern altered the cytoskeletal structure, which changed the quality of cell adhesion in terms of cell adhesion force and cell adhesion strength. The quality of cell adhesion affects cell proliferation. The surface morphology thus affects the cell shape, adhesion force, and proliferation. The strength of cell adhesion is considered a reliable measurement for cytocompatibility.

Acknowledgments This study was supported by the National Science Council, Taiwan, under grant NSC-96-2221-E-006-277.

References

1. Attard NJ, Zarb GA. Immediate and early implant loading protocols: a literature review of clinical studies. J Prosthet Dent. 2005;94(3):242–58.
2. Lin JM, Donahue HJ. Cell sensing and response to micro- and nanostructured surfaces produced by chemical and topographic patterning. Tissue Eng. 2007;13:1879–91.
3. Yim KF. Nanopattern-induced changes in morphology and motility of smooth muscle cells. Biomaterials. 2005;26:5405–13.
4. Chou L, Firth JD, Uitto VJ, Brunette DM. Effects of titanium substratum and grooved surface topography on metalloproteinase-2 expression in human fibroblasts. J Biomed Mater Res. 1998;39:437–45.
5. Werb Z, Hembry RM, Murphy G, Aggeler J. Commitment to expression of metalloendopeptidases, collagenase and stromelysin: relationship of inducing events to changes in cytoskeletal architecture. J Cell Biol. 1986;102:697–702.
6. Watt FM, Jordan PW, O'Neill CH. Cell shape controls terminal differentiation of human epidermal keratinocytes. Proc Natl Acad Sci USA. 1988;85:5576–80.

7. Chen CS, Mrksich M, Huang S, Whitrsides GM, Ingber DE. Micropatterned surface for control of cell shape, position, and Function. Biotechnol Prog. 1998;14:356–63.
8. Chen CS, Mrksich M, Huang S, Whitesides GM, Ingber DE. Geometric control of cell life and death. Science. 1997;276: 1425–8.
9. Schneider GB, Perinpanayagam H, Clegg M, Zaharias R, Seabold D, Keller J, Stanford C. Implant surface roughness affects osteoblast gene expression. J Dent Res. 2003;82:372–6.
10. Le Guehennec L, Soueidan A, Layrolle P, Amouriq Y. Surface treatments of titanium dental implants for rapid osseointegration. Dent Mater. 2007;23:844–54.
11. Benoit M, Gaub HE. Measuring Cell adhesion Forces with the Atomic Force Microscope at the Molecular level. Cells Tissue Organs. 2002;172:174–89.
12. Dalby M. Changes in fibroblast morphology in response to nanocolumns produced by colloidal lithography. Biomaterials. 2004; 25:5415–22.
13. Anselme K. Osteoblast adhesion on biomaterials. Biomaterials. 2000;21:667–81.
14. Reyes CD, Garcia AJ. A centrifugation cell adhesion assay for high-throughput screening of biomaterials surfaces J. Biomed Mater Res. 2003;67A:328–33.
15. Furukawa KS, Ushida T, Nagase T, Nakamigawa H, Noguchi T, Tamaki T, Tanaka J, Tateishi T. Quantitative analysis of cell detachment by shear stress. Mater Sci Eng C. 2001;17:55–8.
16. Athanasiou KA, Thoma BS, Lanctot DR, Shin D, Agrawal CM, LeBaron RG. Development of the cytodetachment technique to quantify mechanical adhesiveness of the single cell. Biomaterials. 1999;20:2405–15.
17. Yamamoto A, Mishima S, Maruyama N, Sumita M. Quantitative evaluation of cell attachment to glass, polystyrene, and fibronectin-or collagen-coated polystyrene by measurement of cell adhesive shear force and cell detachment energy J. Biomed Mater Res. 2000;50:114–24.
18. Wang CC, Hsu YC, Su FC, Lu SC, Lee TM. Effects of passivation treatments on titanium alloy with nano-metric scale roughness and induced changes in fibroblast initial adhesion evaluated by a cytodetacher. J Biomed Mater Res. 2009;88A: 370–87.
19. Comella BT, Scanlon MR. The determination of the elastic modulus of microcantilever beams using atomic force microscopy. J Mater Sci. 2000;35:567–72.
20. Curtis A, Wilkinson C. Topographical control of cells. Biomaterials. 1997;18:1573–83.
21. Wan Y, Wang Y, Liu Z, Qu X, Han B, Bei J, Wang S. Adhesion and proliferation of OCT-1 osteoblast-like cells on micro- and nano-scale topography structured poly(L-lactide). Biomaterials. 2005;26:4453–9.
22. Abrams G, Goodman SL, Nealey PF, Franco M, Murphy CJ. Nanoscale topography of the basement membrane underlying the corneal epithelium of the Rhesus Macaque. J Cell Sci. 2004; 117:3153–64.
23. Liu X, Lim JY, Donahue HJ, Dhurjati R, Mastro AM, Vogler EA. Influence of substratum surface chemistry/energy and topography on the human fetal osteoblastic cell line hFOB1.19: phenotypic and genotypic responses observed in vitro. Biomaterials. 2007; 28:4535–50.
24. Thevenot P, Hu W, Tang L. Surface chemistry influences implant biocompatibility. Curr Top Med Chem. 2008;8:270–80.
25. Bodhak S, Bose S, Bandyopadhyay A. Role of surface charge and wettability on early stage mineralization and bone cell–materials interactions of polarized hydroxyapatite. Acta Biomater. 2009;5: 2178–88.
26. Schneider G, Burridge K. Formation of focal adhesions by osteoblasts adhering to different substrata. Exp Cells Res. 1994; 214:264–9.
27. Uttayarat P, Toworfe GK, Dietrich F, Lelkes PI, Composto RJ. Topographic guidance of endothelial cells on silicone surfaces with micro- to nanogrooves: orientation of actin filaments and focal adhesions. J Biomed Mater Res. 2005;75A:668–80.
28. Chesmel KD, Clark CC, Brighton CT, Black J. Cellular responses to chemical and morphologic aspects of biomaterial surfaces, II. The biosynthetic and migratory response of bone cell populations. J Biomed Mater Res. 1995;29:1101–10.
29. Balaban NQ, et al. Force and focal adhesion assembly: a close relationship studied using elastic micropatterned substrates. Nat Cell Biol. 2001;3(5):466–72.
30. Kelly S, Regan EM, Uney JB, Dick AD, McGeehan JP, Mayer EJ, Claeyssens F. Patterned growth of neuronal cells on modified diamond-like carbon substrates. Biomaterials. 2008;29(17):2573–80.
31. Teixeira AI, Abrams GA, Bertics PJ, Murphy CJ, Nealey PF. Epithelial contact guidance on well-defined micro- and nanostructured substrates. J Cell Sci. 2003;116:1881–92.
32. Falconnet D, Csucs G, Grandin HM, Textor M. Surface engineering approaches to micropattern surfaces for cell-based assays. Biomaterials. 2006;27:3044–4063.
33. Walboomers XF, Monaghan W, Curtis ASG, Jansen JA. Attachment of fibroblast on smooth and microgrooved polystyrene. J Biomed Mater Res. 1999;46:212–20.
34. Chou L, Firth JD, Uitto VJ, Brunette DM. Substratum surface topography alters cell shape and regulates fibronectin mRNA level, mRNA stability secretion and assembly in human fibroblasts. J Cell Sci. 1995;108:1563–73.
35. Yamamoto A, Mishima S, Maruyama N, Sumita M. A new technique for direct measurement of the shear force necessary to detach a cell from a material. Biomaterials. 1998;19:871–9.
36. Wang CC, Hsu YC, Hsieh MC, Yang SP, Su FC, Lee TM. Effects of nano-surface properties on initial osteoblast adhesion and Ca/P adsorption ability for titanium alloys. Nanotechnology. 2008; 19:335709–18.
37. Garcia AJ, Ducheyne P, Boettiger D. Quantification of cell adhesion using a spinning disc device and application to surface-reactive materials. Biomaterials. 1998;18:1091–8.
38. Kim YJ, Shin JW, Park K, Lee JW, Yui N, Park SA, Jee KS, Kim JK. A study of compatibility between cells and biopolymeric surfaces through quantitative measurements of adhesive forces. J Biomater Sci Polym Ed. 2003;14:1311–21.